Running Title: Establishment of endometrial cell line

Establishment and characterization of cell lines from human endometrial epithelial and mesenchymal cells from patients with endometriosis

Ayako Muraoka, MD[a,b], Satoko Osuka, MD, PhD[a,*], Tohru Kiyono, MD, PhD[c], Miho Suzuki, PhD[b], Akira Yokoi, MD, PhD[a], Tomohiko Murase, MD, PhD[a], Kimihiro Nishino, MD, PhD[a], Kaoru Niimi, MD, PhD[a], Tomoko Nakamura, MD, PhD[a], Maki Goto, MD, PhD[a], Hiroaki Kajiyama, MD, PhD[a], Yutaka Kondo, MD, PhD[b], and Fumitaka Kikkawa, MD, PhD[a]

[a] Department of Obstetrics and Gynecology, Nagoya University Graduate School of Medicine, 65 Tsurumai-cho, Showa-ku, Nagoya 466-8550, Japan

[b] Division of Cancer Biology, Nagoya University Graduate School of Medicine, 65 Tsurumai-cho, Showa-ku, Nagoya 466-8550, Japan

[c] Project for Prevention of HPV-related Cancer, Exploratory Oncology Research & Clinical Trial Center, National Cancer Center, Kashiwanoha 6-5-1, Kashiwa City, Chiba Pref. 277-8577, Japan

***corresponding author**: Satoko Osuka

Department of Obstetrics and Gynecology, Nagoya University Graduate School of Medicine, 65 Tsurumai-cho, Showa-ku, Nagoya 466-8550, Japan

Telephone: +81-52-744-2261; Fax: +81-52-744-2268

e-mail: satokoosuka@med.nagoya-u.ac.jp

Capsule: Novel immortalization methods allow us to establish suitable endometrial epithelial and mesenchymal cell lines from patients with or without endometriosis.

Abstract

Objective: To establish and characterize cell lines derived from human endometrial epithelial cells (ECs) and mesenchymal cells (MCs) from patients with and without endometriosis.

Design: In vitro experimental study

Setting: University and National Cancer Center Research Institute

Patients: Two women with endometriosis and two women without endometriosis

Intervention(s): Sampling of endometrial ECs and MCs

Main Outcome Measure(s): We established immortalized endometrial ECs and MCs. Quantitative reverse transcription-polymerase chain reaction (qRT-PCR), immunocytochemical analysis, and RNA sequence profiling were performed to characterize immortalized cells. A cell proliferation assay, three-dimensional culture, and assays for hormonal responses were performed to characterize the features of ECs.

Results: qRT-PCR, immunocytochemical analysis, and western blotting revealed that ECs and MCs maintained their original features. Moreover, immortalized cells were found to retain responsiveness to sex steroid hormones. ECs formed a gland-like structure in 3D culture, indicating the maintenance of normal EC phenotypes. RNA sequence profiling, principal component analysis, and clustering analysis showed that the gene expression patterns of immortalized cells were different from those of cancer cells. Several signaling pathways that were significantly enriched in ECs and MCs with endometriosis were revealed.

Conclusion: We successfully obtained four paired immortalized endometrial ECs and MCs from patients with and without endometriosis. Using these cells could help identify diagnostic and therapeutic targets for endometriosis. The cell lines established in this study will thus serve as powerful experimental tools in the study of endometriosis.

Keywords: endometrial cells, endometriosis, epithelial cells, mesenchymal cells, immortalization

Introduction

Endometriosis is characterized by the presence of the endometrium outside the uterine cavity, causing chronic pelvic pain and infertility (1). To date, several hypotheses, such as retrograde menstruation, coelomic metaplasia, and Müllerian remnants, have been proposed as a cause of endometriosis (2-6), for example, although most women of reproductive age exhibit some degree of retrograde menstruation, not every woman develops endometriosis, suggesting that unknown underlying mechanisms may be responsible for the development of endometriosis. To examine the mechanisms that contribute to endometriosis, several studies have been performed to investigate differentially expressed genes in epithelial cells (ECs) and mesenchymal cells (MCs) of the endometrium from patients with and without endometriosis (7–9). On these previous studies, ECs were collected by laser capture microdissection or mixed RNA was extracted from each whole-tissue specimen. Isolated ECs were used directly and were not cultured prior to expression profiling. An appropriate model of endometriosis that could culture in vitro and reflect their original characters is lacking, especially no paired primary ECs and MCs from the same patients have not been established so far. Because of the lack of these suitable models of endometriosis, the precise mechanism of this disease has not been sufficiently investigated.

As the number of passages of primary endometrial cells is limited in standard culture conditions, it is necessary to establish immortalized endometrial cell lines as a suitable in vitro model. It is known that the senescence of primary endometrial cells is caused by the activation of retinoblastoma (RB) and telomere shortening. We developed an advanced medium and used telomerase reverse transcriptase (TERT) to activate telomerase, mutant cyclin-dependent kinase (CDK4), and cyclin D1 to inactivate the pRB pathway, respectively.

Using these four established paired ECs and MCs from the same patients, we characterized these

cells in detail. Our established cell lines are powerful experimental tools for investigating endometriosis.

Materials and Methods

Clinical Samples and Cell Dispersion

Human endometrial samples were obtained from four different patients, and their backgrounds are described in Supplementary Table 1. All patients had regular menstrual periods and did not receive any hormonal treatment for at least 3 months before surgery. This study was approved by the Institutional Review Board of the Nagoya University Graduate School of Medicine (no. 2017-0503); informed consent was obtained from each patient before sampling. The endometrium was obtained with a curette, and the tissue was minced into small pieces in HBSS (14175-079, Gibco) with 30 mM EDTA (pH 6.4) and shaken for 30 min at 37°C. Individual glands were collected under a microscope, and the remaining tissues were shaken for another 30 min at 37°C in Dulbecco's modified Eagle's medium (DMEM) / F12 medium containing 200 U/mL collagenase (Gibco Invitrogen) and then strained through a 40-μm cell-strainer nylon mesh.

Vector Construction and Lentiviral Infection

Lentiviral vectors expressing TERT, cyclin D1, and mutant CDK4 (CDK4R24C: an inhibitor-resistant form of CDK4) were constructed by recombination with a lentiviral vector, CSII-TRE-Tight-RfA or CSII(loxP)-TRE-Tight-RfA (10). CSII-TRE-Tight-RfA was generated by replacing the elongation factor promoter in CSII-EF-RfA with the tetracycline-responsive promoter from pTRE-Tight (Clontech) as described previously (10). CSII (loxP)-TRE-Tight-RfA was generated by inserting a loxP site in the repetitive sequence of 3′-LTR of the vector using PCR with

forward primer, 5′-CataacttcgtataatgtatgctatacgaagttatCTGTACTGGGTCTCTCTGGTTAG-3′, and reverse primer, 5′-AATTCTGCAGCTCTCGGGCCATGTGAT-3′, followed by the In-Fusion reaction (TAKARA). CSII-CMV-tetOff-Adv was generated by recombination of CSII-CMV-RfA and pENTR221-tetOff Adv, which was generated by recombination of the tetOff segment amplified from pTet-Off Advanced with the forward primer, 5′-GGGGACAAGTTTGTACAAAAAAGCAGGCTgccaccATGTCTAGACTGGACAAG-3′ and reverse primer, 5′-GGGGACCACTTTGTACAAGAAAGCTGGGttaCCCGGGGAGCATGTCAA-3′ with pDONR221 by using the Gateway system (ThermoFisher Scientific).

The EpCAM promoter (-1071-+86) amplified from pE39 plasmid (11) with the forward primer, 5′-gcctcgagATCTGCACGGAAATCGATTA-3′, and reverse primer, 5′-ggaattcAGCGCGAGGCCTGGGGCAC-3′, and digested with XhoI and EcoRI was inserted between the XhoI and EcoRI sites of pTet-Off Advanced (TAKARA) to generate pEpCAMp-Tet-OFF Adv. The EpCAM promoter and tetOff segment were then amplified with the forward primer, 5′-recombined with pDONR221, and then recombined with CSII-RfA to generate CSII-EpCAMp-tetOff. CSII-RfA was generated from CSII-EF-RfA by digestion with AgeI followed by self-ligation. The production of recombinant lentiviruses was as detailed earlier (10).

Immortalization of Endometrial ECs and MCs

Primary cells from the glands were plated on a Matrigel-coated 6-well plate with the B medium (12) supplemented with 10 nM 17β-estradiol, 2 mM N-acetyl cysteine, and 200 μM ascorbic acid 2-phosphate 3Na, but lacking nicotinamide. First, at passage 1, cells were infected with the recombinant lentiviruses at a multiplicity of infection of 5. Individual lines were infected with a

combination of lentiviruses listed in Supplementary Table 2. Second, to obtain EC population, contaminated non-ECs were removed. Briefly, EpCAM-positive cells were enriched with CD326 microbeads (Myltenyl Biotec) and/or fibroblasts were depleted by anti-fibroblast microbeads (Myltenyl Biotec) according to the manufacturer's instructions. Lastly, to preferentially propagate EC, we used B medium.

Next, MC lines were established by infecting CSII-CMV-CDK4R24C, CSII-PGK-Cyclin D1, and CSII-CMV-TERT and maintained in DMEM / F12 medium supplemented with 10% (v/v) fetal bovine serum (FBS). After seeding separated cells, we transfected immortalized genes and purified MC populations using anti-fibroblast microbeads (Myltenyl Biotec) per the manufacturer's instructions.

Quantitative Reverse Transcription-Polymerase Chain Reaction

Total RNA was isolated from ECs and MCs using the RNeasy Mini Kit (Qiagen) according to the manufacturer's protocol. cDNA was generated from 1 μg of RNA using Prime Script RT Master Mix (Takara, Kusatsu, Japan). The primers used for amplification are listed in Supplementary Table 3. TaqMan qPCR (Roche Diagnostics, Basel, Switzerland) and SYBR Green qPCR (TOYOBO, Osaka, Japan) were performed in triplicate for the target genes. Gene expression levels were normalized to GAPDH expression levels.

Immunocytochemistry

ECs and MCs were cultured on chamber glass and fixed with 2% paraformaldehyde for 10 min. After incubating with 0.1% Triton X-100 on ice for 2 min, the cells were blocked for 15 min using 2% gelatin. These samples were washed with PBS/glycine and incubated with primary antibody

against CK8/18 (1:50 MM-1007-01; Immunobioscience), E-cadherin (1:50 sc-8426; Santa Cruz Biotechnology, Santa Cruz, CA), vimentin (1:50 sc-6260; Santa Cruz Biotechnology, Santa Cruz, CA), or fibronectin (1:200 ab2413; abcam), or with control serum for 1 hour at room temperature. Following washes with PBS, cells were incubated with DAPI and Alexa Fluor 488-labeled anti-mouse secondary antibody (1:500 A-11029; Thermo Fisher) for CK8/18, E-cadherin, and vimentin and with Alexa Fluor 546-labeled anti-rabbit secondary antibody (1:500 A-11010; Thermo Fisher) for fibronectin for 45 min at room temperature. The expression of each protein was detected using fluorescence microscopy (Leica DFC 9000 GT) under the same condition. Fluorescence intensity of five fields were randomly selected and calculated the mean level of intensity using Image J.

MTT Assay

Cells were seeded at 1×10^3 cells/well in 96-well plates. To compare the cell growth with or without doxycycline, we performed the MTT assay using the Cell Counting Kit-8 (CK04 Dojindo, Japan) according to the manufacturer's protocol. The concentration of doxycycline was 1 mg/mL.

Three-dimensional Culture and Immunohistochemistry

The three-dimensional culture was performed as described previously (13). Briefly, 1×10^5 cells/well were seeded on 100 μL Matrigel (356234 Corning Matrigel Matrix basement membrane, Life Science) mixed with 100 μL DMEM/F12 in a 24-well plate and incubated at 37°C in a 5% CO_2 atmosphere. After 7 days, to confirm the formation of glandular-like structures, colonies were compacted using iPGell (PG20-1 GenoStaff), and formalin-fixed paraffin-embedded sections were prepared. After de-paraffinization and blocking in methanol and 0.3% H_2O_2, specimens were

incubated with the primary antibody against CK8/18 (1:50 MM-1007-01; Immunobioscience) or CD10 (1:50 sc-7632; Santa Cruz Biotechnology, Santa Cruz, CA) overnight at 4°C. After subsequent incubation with HRP-conjugated secondary antibody, specimens were subjected to DAB (DAB, Dako) and hematoxylin staining.

Western Blot Analysis

Western blotting was conducted as described previously (14). Whole-cell protein extracts were used for analysis, and immunoblotting was conducted as described previously (15). Antibodies against cyclin D1 (clone G124-326; BD Biosciences), CDK4 (clone 97; BD Biosciences), E-cadherin (clone 36; BD Biosciences), estrogen receptor (sc-8002; Santa Cruz), progesterone receptor (A00098; DAKO) and GAPDH (AM4300; Ambion) were used as probes, and horseradish peroxidase-conjugated anti-mouse or anti-rabbit (Jackson Immunoresearch Laboratories) immunoglobulins were used as secondary antibodies. The LAS3000 CCD-Imaging System (Fujifilm Co. Ltd., Tokyo, Japan) was used to detect proteins visualized using the Lumi-light plus western blotting substrate (Roche, Basel, Switzerland). Quantification is presented as pixel intensity of each protein normalized to loading control (GAPDH) using Image J.

Assessment of Hormonal Response

To assess the hormonal response, 5×10^3 cells/well were seeded in a 6-well plate and incubated with phenol red-free medium (DMEM high glucose Sigma Aldrich) supplemented with 10% GIBCO Charcoal-stripped FBS (12676-011 Invitrogen) and L-glutamine (G7513 Sigma Aldrich). The cells were then treated with each sex steroid hormone for different time periods. We used 10^{-9} M to 10^{-7} M 17β estradiol (E2) (3301-1GMCN Merck) or 10^{-7} M to 10^{-5} M progesterone (P4)

(P8783-1G Sigma Aldrich) for each experiment and then counted the number of cells.

RNA Sequencing and Data Deposition

Total RNA was isolated from ECs and MCs using the RNeasy Mini Kit (Qiagen). RNA integrity was confirmed using a NanoDrop spectrophotometer and Agilent Bioanalyzer 2100. Sequencing was performed on a Hiseq2000 instrument (Illumina). We mapped the reads to a reference genome (Human, NCBI GRCh38) using Hisat2 (version 2.1.0) (16) with the default settings. The relative gene expression levels were estimated by fragments per kilobase of transcript per million mapped reads (FPKM) using Stringtie (version 1.3.5) (17) with the default settings. We used Genespring (version 14.9, Agilent) for the expression analysis. These data were deposited in the DDBJ BioProject database under accession number E-GEAD-314.

Statistical Analysis

Statistically significant were determined using a two-sided Student's t-test. All experiments were performed in triplicate. $P < 0.05$ was considered statistically significant. Differentially expressed genes obtained from RNA sequence profiling were analyzed using Genespring (version 14.9, Agilent). Genes with a fold change (FC) >2.0 were identified as differentially regulated.

Results

Characterization of ECs and MCs

Human endometrial samples were obtained from four patients (Fig 1A). ECs showed a small round shape and proliferated to form cobblestone-shaped colonies, whereas MCs were spindle-shaped and easily distinguishable from ECs. (Fig 1C). To determine the origin of these immortalized cells, we performed qPCR and immunocytochemistry for EC and MC markers. ECs were positive for cytokeratin 8 and E-cadherin, but negative for vimentin and fibronectin. In contrast, MCs were strongly positive for mesenchymal markers and negative for EC markers (Fig 1B and 1C). To confirm that EC kept the original expression of epithelial markers, we validated the mRNA expression compared to primary EC (before transfection) and immortalized EC (after transfection) (Supplementary Fig 1A). ECs demonstrated higher expression levels of EC marker genes than normal fibroblast cell line (WI38), and the expression levels of the EC marker were almost similar between primary EC and immortalized EC. These results indicated that we succeeded in establishing four pairs of immortalized endometrial ECs and MCs.

Role of Immortalization Genes in the Growth of ECs (Tet-off System)

To search the function of transfected genes, ECs were examined for protein expression and proliferation activity in the presence and absence of doxycycline to confirm that cell growth is dependent on the three transfected genes, mutant CDK4, cyclin D1, and TERT. After incubation with doxycycline for 24 h, the expression levels of mutant CDK4 and cyclin D1 decreased (Fig 2A) and the proliferation was inhibited (Fig 2B), suggesting that proliferation of ECs depended on these transgenes.

Three-dimensional Culture

Three-dimensional (3D) culture was performed to confirm the ability of EC1 and MC1 to reconstruct the morphological characteristics of the original tissues, such as the gland-like structure of ECs or mesh-like formation of MCs. EC1, EC3, MC1, and Ishikawa cells (endometrial adenocarcinoma cell line) were seeded onto Matrigel, and after 7 days, EC1 and EC3 formed gland-like structures, whereas MC1 and Ishikawa cell did not form gland-like structures (Fig 2C). The gland-like formations were positive for cytokeratin but negative for CD10, indicating that these cells were not of mesenchymal origin (Fig 2D). Thus, EC1 and EC3 maintained their ability to reconstruct gland-like structures, different from cancer cell lines. These results indicated that EC1 and EC3 did not acquire an oncogenic phenotype.

Expression of Hormone Receptors and Responsiveness to Sex steroid Hormones

ECs were confirmed to express more estrogen receptor α and progesterone receptors than MCs using western blotting (Fig 3A). We also examined the responsiveness of each immortalized cell line to sex steroid hormones (Fig 3B). Treatment with 17β estradiol significantly promoted the growth of EC1 and EC3 on day 9. In contrast, progesterone treatment significantly inhibited the growth of EC1 and EC3. This indicated that ECs retained their ability to respond to sex steroid hormones.

RNA Sequencing Analysis

For further insight, we examined the global gene expression profile of our immortalized cell lines. First, to characterize the gene expression pattern of immortalized cells compared to that of normal or cancer cells, we profiled the transcriptome of each type of cell by principal component analysis

and clustering analysis. We used available public datasets as normal fibroblasts (GSE 99949), endometrial cancer (GSE 10619), and uterine sarcoma (GSE 64763). Analysis of the results revealed that immortalized cells exhibited different gene expression signatures compared to those of cancer cells (Fig 4A, B). Indeed, ECs and MCs were separated into the different clusters, which justify the identification of ECs and MCs.

Next, we performed pathway analysis for differentially expressed genes to annotate the function of genes from ECs and MCs with endometriosis. Of 57351 genes, 830 genes were upregulated, and 1064 genes were downregulated in ECs with endometriosis compared to those without endometriosis ($FC > 2$, $P < 0.05$). Further, 395 genes were upregulated, and 324 genes were downregulated in MCs with endometriosis compared to those without endometriosis ($FC > 2$, $P < 0.05$). The top 30 upregulated or downregulated genes are listed in Supplementary Table 4 to 7. We then used these significant differentially expressed gene sets for pathway analysis. Of the 1024 pathways, 49 signaling pathways were significantly enriched in ECs with endometriosis, and nine pathways were significantly enriched in MCs with endometriosis (Fig 4C, all pathways were enriched $P < 0.01$). Among the pathways in MCs, the myometrial relaxation and contraction pathway, focal adhesion, and matrix metalloproteinase (MMPs) were enriched. These pathways have already been reported previously and are known to be associated with the endometriosis pathophysiology (18–23). In contrast, among the pathways of the ECs, different pathways were enriched compared to those in MCs, except for those related to focal adhesion and MMPs. Several pathways, including the Wnt signaling pathway, TGF-β signaling pathway, and MAPK signaling pathway, which have been already reported as endometriosis-related pathways in MC research (7,27,28,33–37), were also found to be enriched in ECs with endometriosis.

Discussion

In this study, we established four paired immortalized ECs and MCs from patients with and without endometriosis to provide a resource that helps reveal the mechanism of onset of endometriosis. Our approach consists of three advantages in the establishment process. First, although primary ECs cannot be sustained for several days under standard culture condition, a sufficient quantity of endometrial ECs is required for immortalization processes. Therefore, we used an original conditional medium, which allowed us to acquire sufficient ECs with a minimum number of passages. The modified medium included several growth factors, such as Wnt; the BMP inhibitor, noggin; and the Wnt agonist, R-spondin, which are indispensable for EC proliferation. Particularly, activation of the Wnt pathway confers effective growth of ECs. A previous study reported that small intestinal ECs require Wnt factors in culture because of the low concentration of Wnt ligands in the epithelial culture medium (12,30). In mouse small intestinal epithelial organoid culture, the asymmetric architecture of organoids collapses due to the loss of the local gradient of Wnt factors (31). These factors are known to be necessary for intestinal EC proliferation; thus, we applied these growth factors to our endometrial ECs.

Second, highly purified ECs are essential for the establishment of immortalized cells, since MCs contaminating an EC population often overwhelm the ECs after several passages because of the difference in their proliferation rates. We used an anti-EpCAM (CD326) antibody-conjugated magnetic bead-based method to purify the ECs. EpCAM is an epithelium-specific but highly abundant epithelial surface marker, even in the endometrium (32–36). Previous animal studies have shown that EpCAM plays an important role in the structural and functional development of the uterine endometrium, as well as in adult uterine function. EpCAM is capable to controlling cell fate by altering directional cell proliferation and differentiation (37–42). EpCAM affects cell signaling

and can activate Wnt signaling by stabilizing transmembrane receptors (43). From this point of view, EpCAM is an essential epithelial marker in the endometrium, and using this marker is suitable for the acquisition of functional ECs. Through the purification process, we successfully enriched EpCAM-positive cells. From our experimental data, ECs maintained the expression level of epithelial markers, EpCAM, E-cadherin, and cytokeratin for 20 passages (data not shown). In this regard, modified culture conditions and purification of ECs are useful for the establishment of suitable immortalized ECs and maintenance of EC features. The combination of these methods allowed us to constantly immortalize normal endometrial ECs.

Third, transfection of genes for immortalization sometimes causes problems, such as the elimination of the original features of the primary cells, and they may gain altered phenotypes (14,15,44,45). We changed the transgenes for immortalization from human papillomavirus 16 (HPV16) E6/E7 to mutant CDK4, cyclin D1, and TERT. We further used an EpCAM promotor-derived expression vector to activate these immortalizing transgenes, specifically in EC2 and EC4 (11). Although HPV16 E6/E7 can efficiently immortalize primary normal cells, E6 targets p53 for degradation, and E6 and E7 oncoproteins independently induce numerical and structural chromosome instability (44). Thus, the immortalized cells tend to lose their original characteristics over a short period of time and gain altered phenotypes. The combination of mutant CDK4, cyclin D1, and TERT has successfully immortalized many human, as well as non-human, primary ECs with minimal induction of chromosomal instability (46–60). CDK4 and cyclin D1 have a direct effect on the inactivation of pRB. Furthermore, as inactivation of the Rb tends to activate p53 through p14ARF, chromosomal stability could further be maintained through passages (44). The original characteristics of our immortalized cells could be validated using the tet-off system. Doxycycline treatment to shut down the transgenes induced strong growth inhibition, indicating

that their original character before transformation could be addressed using this tet-off system.

Our RNA sequencing analysis revealed that the gene expression patterns of ECs and MCs from the endometriosis patients were already different from ECs and MCs from non-endometriosis patients. In our pathway analysis, several signaling pathways that were enriched in ECs and MCs from patients with endometriosis were equivalent to previously reported endometriosis-related pathways, which were revealed by using ectopic fibroblasts from endometriosis lesions (9,24–26,29). Because retrograde menstruation is thought to be one of the major causes of endometriosis, endometriosis-like cells in the eutopic endometrium may contribute to the establishment of endometriosis. Further studies on endometrial cells will be informative to reveal the etiology of endometriosis.

Our study has the limitation that we obtained the endometrial samples from different menstrual cycles. It might have affected the gene expression analysis of the immortalized cells when we evaluated gene expression analysis. Further studies on this topic are required. From our qRT-PCR results, EC1 and EC2 showed higher mRNA expression levels of E-cadherin than EC3 and EC4. These results might be influenced by the hormonal status of each of the cells, because the epithelial mesenchymal transition is increased during secretory phase (61). Still, it is difficult to completely recapture the endometriosis only by this cell line system.

Conclusions

We established four paired immortalized ECs and MCs from patients with and without endometriosis. Our culture system and immortalization method are useful for providing benefits and contributing as experimental tools for further studies on endometriosis.

Acknowledgments

We would like to thank Ms. Chiho Kohno (NCCRI) for technical assistance. We are also grateful to Dr. Marianne G. Rots (University of Groningen) for providing pE39 plasmid and Dr. Hiroyuki Miyoshi (Riken BioResource Center, present affiliation: Keio University) for providing the lentivirus plasmids, and its packaging system. This work was supported by the Grant-in-Aid for Scientific Research 7120K09615 to Tomoko Nakamura from the Japan Society for the Promotion of Science, Japan.

References

1. Giudice LC. Endometriosis. N Engl J Med 2010;362:2089–98.

2. Sampson JA. Peritoneal endometriosis due to the menstrual dissemination of endometrial tissue into the peritoneal cavity. Am J Obstet Gynecol 1927;14:422–69.

3. Vinatier D, Orazi G, Cosson M, Dufour P. Theories of endometriosis. Eur J Obstet Gynecol Reprod Biol 2001;96: 21–34.

4. Redwine DB. Mülleriosis. The single best-fit model of origin of endometriosis. J Reprod Med 1988;33:915-20.

5. Montgomery GW, Mortlock S, Giudice LC. Should genetics now be considered the pre-eminent etiologic factor in endometriosis? J Minim Invasive Gynecol 2020;27:280-6.

6. Redwine DB. Is "microscopic" peritoneal endometriosis invisible? Fertil Steril 1988;50:665-6.

7. Chand AL, Murray AS, Jones RL, Hannan NJ, Salamonsen LA, Rombauts L. Laser capture microdissection and cDNA array analysis of endometrium identify CCL16 and CCL21 as epithelial-derived inflammatory mediators associated with endometriosis. Reprod Biol Endocrinol 2007;5:1–13.

8. Burney RO, Talbi S, Hamilton AE, Kim CV, Nyegaard M, Nezhat CR, et al. Gene expression analysis of endometrium reveals progesterone resistance and candidate susceptibility genes in women with endometriosis. Endocrinology 2007;148:3814–26.

9. Matsuzaki S, Canis M, Vaurs-Barrière C, Boespflug-Tanguy O, Dastugue B, Mage G. DNA microarray analysis of gene expression in eutopic endometrium from patients with deep endometriosis using laser capture microdissection. Fertil Steril 2005;84:1180–90.

10. Inagawa Y, Yamada K, Yugawa T, Ohno SI, Hiraoka N, Esaki M, et al. A human cancer xenograft model utilizing normal pancreatic duct epithelial cells conditionally transformed with

defined oncogenes. Carcinogenesis 2014;35:1840–6.

11. McLaughlin PMJ, Trzpis M, Kroesen BJ, Helfrich W, Terpstra P, Dokter WHA, et al. Use of the EGP-2/Ep-CAM promoter for targeted expression of heterologous genes in carcinoma derived cell lines. Cancer Gene Ther 2004;11:603–12.

12. Ghani, Dendo, Watanabe, Yamada, Yoshimatsu, Yugawa, et al. An ex-vivo culture system of ovarian cancer faithfully recapitulating the pathological features of primary tumors. Cells 2019;8:644. 13. Arnold JT, Kaufman DG, Seppälä M, Lessey BA. Endometrial stromal cells regulate epithelial cell growth in vitro: A new co-culture model. Hum Reprod 2001;16:836–45.

14. Yugawa T, Handa K, Narisawa-Saito M, Ohno S, Fujita M, Kiyono T. Regulation of notch1 gene expression by p53 in epithelial cells. Mol Cell Biol 2007;27:3732–42.

15. Narisawa-Saito M, Inagawa Y, Yoshimatsu Y, Haga K, Tanaka K, Egawa N, et al. A critical role of MYC for transformation of human cells by HPV16 E6E7 and oncogenic HRAS. Carcinogenesis 2012;33:910–7.

16. Kim D, Langmead B, Salzberg SL. HISAT: a fast spliced aligner with low memory requirements. Nat Methods [Internet] 2015;12:357. Available at: https://doi.org/10.1038/nmeth.3317

17. Pertea M, Kim D, Pertea GM, Leek JT, Salzberg SL. Transcript-level expression analysis of RNA-seq experiments with HISAT, StringTie and Ballgown. Nat Protoc [Internet] 2016;11:1650. Available at: https://doi.org/10.1038/nprot.2016.095

18. Sui X, Li Y, Sun Y, Li C, Li X, Zhang G. Expression and significance of autophagy genes LC3, beclin1 and MMP-2 in endometriosis. Exp Ther Med 2018;16:1958–62.

19. Kalluri R, Weinberg RA, Sonderegger S, Pollheimer J, Knöfler M, Cervelló I, et al. Enhancer of Zeste homolog 2 (EZH2) induces epithelial-mesenchymal transition in endometriosis. Fertil Steril

2018;9:1–11.

20. Mu L, Ma YY. Expression of focal adhesion kinase in endometrial stromal cells of women with endometriosis was adjusted by ovarian steroid hormones. Int J Clin Exp Pathol 2015;8:1810–5.

21. Meola J, Rosa e Silva JC, Dentillo DB, da Silva WA, Veiga-Castelli LC, de Souza Bernardes LA, et al. Differentially expressed genes in eutopic and ectopic endometrium of women with endometriosis. Fertil Steril 2010;93:1750–73.

22. Zhang Q, Duan J, Olson M, Fazleabas A, Guo SW. Cellular changes consistent with epithelial-mesenchymal transition and fibroblast-to-myofibroblast transdifferentiation in the progression of experimental endometriosis in baboons. Reprod Sci 2016;23:1409–21.

23. Zhang Q, Duan J, Liu X, Guo S. Molecular and Cellular Endocrinology Platelets drive smooth muscle metaplasia and fibrogenesis in endometriosis through epithelial-mesenchymal transition and fibroblast-to-myofibroblast transdifferentiation. Mol Cell Endocrinol 2016;428:1–16.

24. Liu Z, Yi L, Du M, Gong G, Zhu Y. Overexpression of TGF-β enhances the migration and invasive ability of ectopic endometrial cells via ERK/MAPK signaling pathway. Exp Ther Med 2019;4457–64.

25. Young VJ, Ahmad SF, Brown JK, Duncan WC, Horne AW. Peritoneal VEGF-A expression is regulated by TGF-β1 through an ID1 pathway in women with endometriosis. Sci Rep 2015;5:1–9.

26. Yotova I, Hsu E, Do C, Gaba A, Sczabolcs M, Dekan S, et al. Epigenetic alterations affecting transcription factors and signaling pathways in stromal cells of endometriosis. 2017；12:1–32.

27. Kao LC, Germeyer A, Tulac S, Lobo S, Yang JP, Taylor RN, et al. Expression profiling of endometrium from women with endometriosis reveals candidate genes for disease-based implantation failure and infertility. Endocrinology 2003;144:2870–81.

28. Pabona JMP, Simmen FA, Nikiforov MA, Zhuang DZ, Shankar K, Velarde MC, et al.

Krüppel-like factor 9 and progesterone receptor coregulation of decidualizing endometrial stromal cells: Implications for the pathogenesis of endometriosis. J Clin Endocrinol Metab 2012;97:376–92.

29. Matsuzaki S, Botchorishvili R, Pouly JL, Canis M. Targeting the Wnt/β-catenin pathway in endometriosis: a potentially effective approach for treatment and prevention. Mol Cell Ther 2014;2:36.

30. Nakamura T, Sato T. Advancing intestinal organoid technology toward regenerative medicine. Cell Mol Gastroenterol Hepatol 2018;5:51–60.

31. Sato T, Van Es JH, Snippert HJ, Stange DE, Vries RG, Van Den Born M, et al. Paneth cells constitute the niche for Lgr5 stem cells in intestinal crypts. Nature 2011;469:415–8.

32. Huang L, Yang Y, Yang F, Liu S, Zhu Z, Lei Z, et al. Functions of EpCAM in physiological processes and diseases. Int J Mol Med 2018;42:1771–85.

33. Ghezzi P. Protein glutathionylation in health and disease. BBA - Gen Subj 2013;1830:3165–72.

34. Masuda A, Katoh N, Nakabayashi K, Kato K, Sonoda K, Kitade M, et al. An improved method for isolation of epithelial and stromal cells from the human endometrium. J Reprod Dev 2016;62;213-8.

35. Chan RWS, Schwab KE, Gargett CE. Clonogenicity of human endometrial epithelial and stromal cells. Biol Reprod 2004;70:1738–50.

36. Jin S. Bipotent stem cells support the cyclical regeneration of endometrial epithelium of the murine uterus. Proc Natl Acad Sci U S A 2019;116:6848–57.

37. Lindberg ME, Stodden GR, King ML, MacLean JA, Mann JL, DeMayo FJ, et al. Loss of cdh1 and Pten accelerates cellular invasiveness and angiogenesis in the mouse uterus. Biol Reprod 2013;89:1–10.

38. Reardon SN, King ML, MacLean JA, Mann JL, DeMayo FJ, Lydon JP, et al. Cdh1 is essential

for endometrial differentiation, gland development, and adult function in the mouse uterus. Biol Reprod 2012;86:1–10.

39. Nagao K, Zhu J, Heneghan MB, Hanson JC, Morasso MI, Tessarollo L, et al. Abnormal placental development and early embryonic lethality in EpCAM-Null mice. PLoS One 2009;4:e8543. doi: 10.1371/journal.pone.0008543.

40. Guerra E, Lattanzio R, la Sorda R, Dini F, Tiboni GM, Piantelli M, et al. mTrop1/Epcam knockout mice develop congenital tufting enteropathy through dysregulation of intestinal E-cadherin/β-catenin. PLoS One 2012;7:e49302. doi: 10.1371/journal.pone.0049302.

41. Lei Z, Maeda T, Tamura A, Nakamura T, Yamazaki Y, Shiratori H, et al. EpCAM contributes to formation of functional tight junction in the intestinal epithelium by recruiting claudin proteins. Dev Biol 2012;371:136–45.

42. Poon CE, Madawala RJ, Day ML, Murphy CR. EpCAM is decreased but is still present in uterine epithelial cells during early pregnancy in the rat: potential mechanism for maintenance of mucosal integrity during implantation. Cell Tissue Res 2015;359:655–64.

43. Lu H, Ma J, Yang Y, Shi W, Luo L. EpCAM Is an endoderm-specific Wnt derepressor that licenses hepatic development. Dev Cell 2013;24:543–53.

44. Duensing S, Münger K. The human papillomavirus type 16 E6 and E7 oncoproteins independently induce numerical and structural chromosome instability. Cancer Res 2002;62:7075–82.

45. Murakami I, Egawa N, Griffin H, Yin W, Kranjec C, Nakahara T, et al. Roles for E1-independent replication and E6-mediated p53 degradation during low-risk and high-risk human papillomavirus genome maintenance. PLoS Pathog 2019;15:e1007755. doi: 10.1371/journal.ppat.1007755.

46. Katayama M, Kiyono T, Kuroda K, Ueda K, Onuma M, Shirakawa H, et al. Rat-derived feeder cells immortalized by expression of mutant CDK4, cyclin D1, and telomerase can support stem cell growth. Biochim Biophys Acta - Mol Cell Res 2019;1866:945–56.

47. Gouko R, Onuma M, Eitsuka T, Katayama M, Takahashi K, Nakagawa K, et al. Efficient immortalization of cells derived from critically endangered Tsushima leopard cat (Prionailurus bengalensis euptilurus) with expression of mutant CDK4, Cyclin D1, and telomerase reverse transcriptase. Cytotechnology 2018;70:1619–30.

48. Tani T, Eitsuka, Katayama, Nagamine, Nakaya Y, Suzuki H, et al. Establishment of immortalized primary cell from the critically endangered Bonin flying fox (Pteropus pselaphon). PLoS One 2019;14:1–19.

49. Shiomi K, Kiyono T, Okamura K, Uezumi M, Goto Y, Yasumoto S, et al. CDK4 and cyclin D1 allow human myogenic cells to recapture growth property without compromising differentiation potential. Gene Ther 2011;18:857–66.

50. Zushi Y, Noguchi K, Urade M. An in vitro multistep carcinogenesis model for both HPV-positive and -negative human oral squamous cell carcinomas. Japanese J Oral Maxillofac Surg 2013;59:159–71.

51. Katayama M, Hirayama T, Kiyono T, Onuma M, Tani T, Takeda S, et al. Immortalized prairie vole-derived fibroblasts (VMF-K4DTs) can be transformed into pluripotent stem cells and provide a useful tool with which to determine optimal reprogramming conditions. J Reprod Dev 2017;63:311–8.

52. Fukuda T, Eitsuka T, Donai K, Kurita M, Saito T, Okamoto H, et al. Expression of human mutant cyclin dependent kinase 4, Cyclin D1 and telomerase extends the life span but does not immortalize fibroblasts derived from loggerhead sea turtle (Caretta caretta). Sci Rep 2018;8:1–15.

53. Orimoto A, Kyakumoto S, Eitsuka T, Nakagawa K, Kiyono T, Fukuda T. Efficient immortalization of human dental pulp stem cells with expression of cell cycle regulators with the intact chromosomal condition. PLoS One 2020;15:1–18.

54. Orimoto A, Katayama M, Tani T, Ito K, Eitsuka T, Nakagawa K, et al. Primary and immortalized cell lines derived from the Amami rabbit (Pentalagus furnessi) and evolutionally conserved cell cycle control with CDK4 and Cyclin D1. Biochem Biophys Res Commun 2020;525:1046–53.

55. Teng Z, Yoshida T, Okabe M, Toda A, Higuchi O, Nogami M, et al. Establishment of immortalized human amniotic mesenchymal stem cells. Cell Transplant 2013;22:267–78.

56. Hashimoto N, Kiyono T, Saitow F, Asada M, Yoshida M. Reversible differentiation of immortalized human bladder smooth muscle cells accompanied by actin bundle reorganization. PLoS One 2017;12:1–27.

57. Fukuda T, Iino Y, Eitsuka T, Onuma M, Katayama M, Murata K, et al. Cellular conservation of endangered midget buffalo (Lowland Anoa, Bubalus quarlesi) by establishment of primary cultured cell, and its immortalization with expression of cell cycle regulators. Cytotechnology 2016;68:1937–47.

58. Hashimoto H, Suda Y, Miyashita T, Ochiai A, Tsuboi M, Masutomi K, et al. A novel method to generate single-cell-derived cancer-associated fibroblast clones. J Cancer Res Clin Oncol 2017;143:1409–19.

59. Kuroda K, Kiyono T, Isogai E, Masuda M, Narita M, Okuno K, et al. Immortalization of fetal bovine colon epithelial cells by expression of human cyclin D1, mutant cyclin dependent kinase 4, and telomerase reverse transcriptase: An in vitro model for bacterial infection. PLoS One 2015;10:1–18.

60. Fukuda T, Iino Y, Onuma M, Gen B, Inoue-Murayama M, Kiyono T. Expression of human cell cycle regulators in the primary cell line of the African savannah elephant (loxodonta africana) increases proliferation until senescence, but does not induce immortalization. Vitr Cell Dev Biol - Anim 2016;52:20–26.

61. Bilyk O, Coatham M, Jewer M, Postivit L. Epithelial-to-mesenchymal transition in the female reproductive tract: from normal functioning to disease pathology. Front Oncol 2017;7:1–21.

Figure Legends

Fig 1

Cell-type-specific markers and morphology of ECs and MCs

(A) The scheme and table of each established endometrial EC and MC line. (B) Quantitative RT-PCR for the determination of mRNA levels of EC marker genes (cytokeratin 8 and E-cadherin) and MC marker genes (vimentin and fibronectin). Values were normalized to GAPDH expression. Data are means ± SD. (C) Morphology and immunocytochemical staining of each marker protein. Magnification, ×100. Scale bars, 200 μm. Bar charts are quantifications of the fluorescence intensity in five different random fields of each cell. Data are means ± SD.

Fig 2

Analysis of immortalization using the Dox-off system.

(A) Immunoblotting to detect CDK4 and cyclin D1 in ECs and MCs. GAPDH was used as the loading control. Dox (+) cell extracts were prepared after incubation with doxycycline for 24 h. Dox indicates doxycycline. Bar charts are quantifications of the relative intensity of each band normalized to GAPDH. The expression level of cyclin D1 or CDK4 of ECs was significantly decreased under doxycycline treatment.

Data are means ± SD. **, $P < 0.01$ by the two-sided Student's t-test.

(B) Proliferation of EC1 and EC3 with or without doxycycline treatment. Data are means ± SD.

Three-dimensional culture of immortalized cells and an endometrial carcinoma cell line (Ishikawa cell).

(C) Photomicrographs of EC1, EC3, MC1, and Ishikawa cells. The dotted line indicates the

gland-like structure. Magnification, ×100. Scale bars, 500 μm

(D) Immunohistochemical staining of EC1 and EC3. Original magnification ×200 and high-power field ×400. Scale bars; 200 μm and 100 μm.

Fig 3

Expression of sex steroid hormone receptors and responsiveness to hormonal treatment

(A) Immunoblotting of estrogen receptor α (ERα) and progesterone receptor (PR-A and PR-B) in ECs and MCs. GAPDH, loading control. Bar charts are quantifications of the relative intensity of each band normalized to GAPDH. Data are means ± SD. **, $P < 0.01$, n.s. stands for 'not significant' by the two-sided Student's t-test.

(B) Proliferation of EC1 and EC3 treated with E2 or P4. Data are means ± SD. *, $P < 0.05$ **, $P < 0.01$ by the two-sided Student's t-test.

Fig 4

Gene expression and functional analysis of ECs and MCs using RNA sequencing.

(A) Principal component analysis of endometrial cell samples. Gene expression data were published on Gene Expression Omnibus. The one dot plot indicates the gene expression data for one patient.

(B) Clustering analysis of endometrial cells. The heatmap shows the gene expression levels. Red indicates low expression level, and blue indicates high expression level.

(C) Pathway analysis of differentially expressed gene sets of ECs and MCs with endometriosis (FC > 2, $P < 0.05$). The X-axis shows the enrichment score (-log10, P value). The Y-axis shows the name of the signaling pathway. The top significantly enriched pathways are indicated ($P < 0.01$).

A

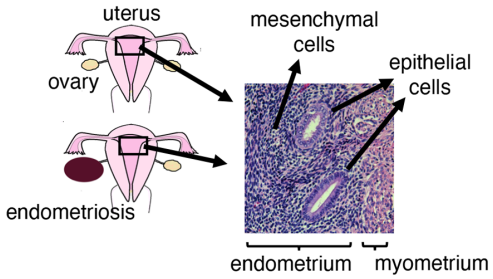

Without Endometriosis	patient 1	patient 2
epithelial cell	EC1	EC2
mesenchymal cell	MC1	MC2

With Endometriosis	patient 3	patient 4
epithelial cell	EC3	EC4
mesenchymal cell	MC3	MC4

B

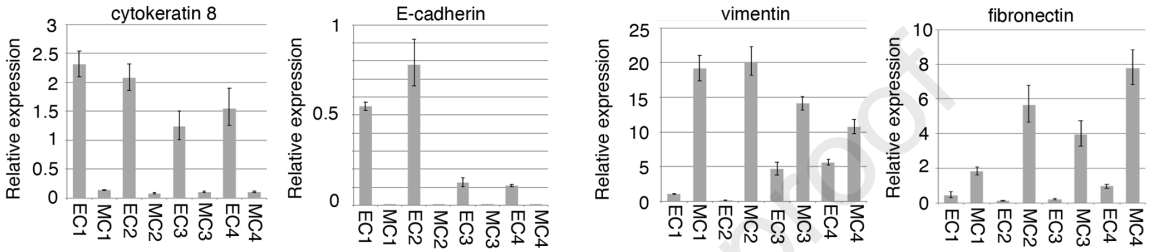

C

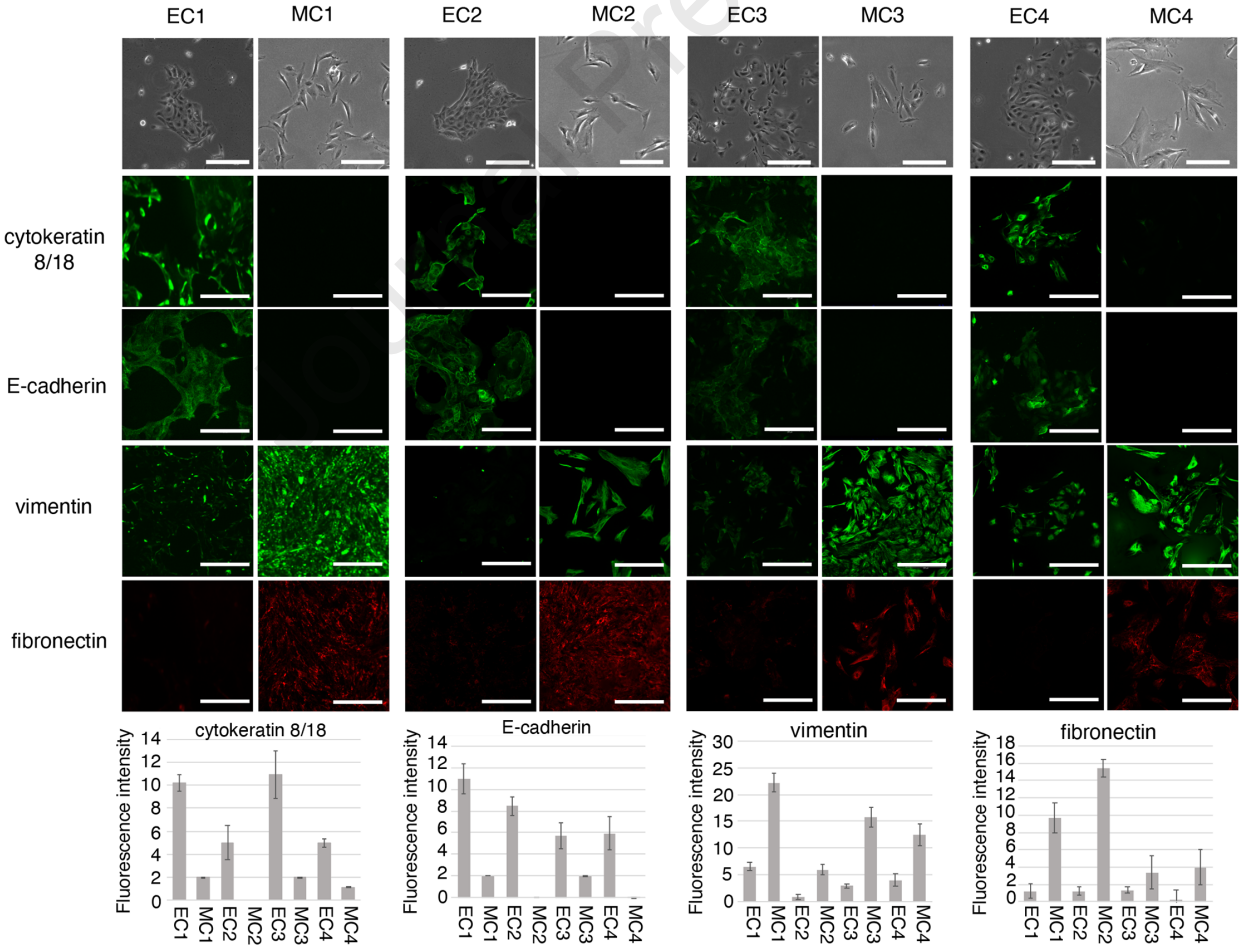

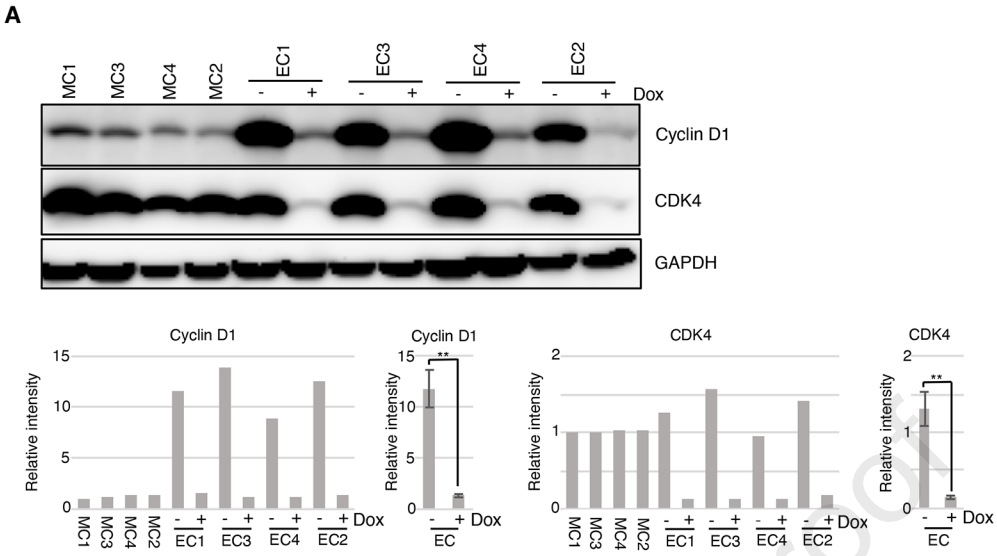
A
MC1
MC3
MC4
MC2
EC1
EC3
EC4
EC2
Dox
Cyclin D1
CDK4
GAPDH
Relative intensity
**

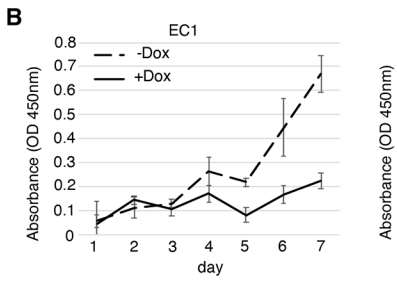
B
EC1
-Dox
+Dox
Absorbance (OD 450nm)
day

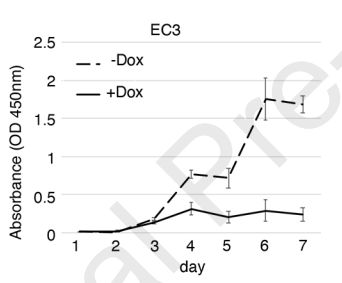
EC3
-Dox
+Dox
Absorbance (OD 450nm)
day

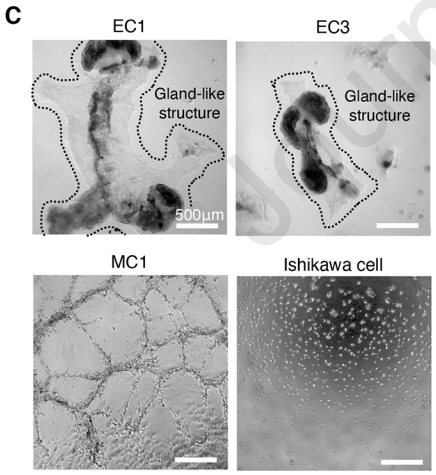
C
EC1
EC3
Gland-like structure
500μm
MC1
Ishikawa cell

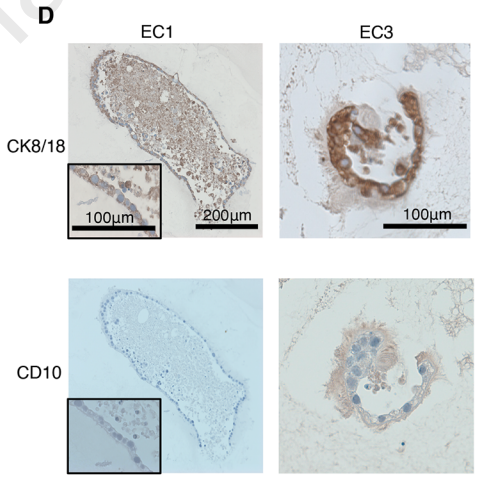
D
EC1
EC3
CK8/18
100μm
200μm
CD10